Vanishing and Revival of Resonance Raman Scattering

Yu Guo (郭裕),[1,2] Chuan-Cun Shu (束传存),[1,3,*] Daoyi Dong,[4] and Franco Nori (野理)[3,5]

[1]Hunan Key Laboratory of Super-Microstructure and Ultrafast Process, School of Physics and Electronics, Central South University, Changsha 410083, China

[2]Hunan Provincial Key Laboratory of Flexible Electronic Materials Genome Engineering, School of Physics and Electronic Science, Changsha University of Science and Technology, Changsha 410114, China

[3]Theoretical Quantum Physics Laboratory, RIKEN, Wako, Saitama 351-0198, Japan

[4]School of Engineering and Information Technology, University of New South Wales, Canberra, Australian Capital Territory 2600, Australia

[5]Physics Department, University of Michigan, Ann Arbor, Michigan 48109, USA

(Received 26 August 2019; published 26 November 2019)

The possibility to manipulate quantum coherence and interference, apart from its fundamental interest in quantum mechanics, is essential for controlling nonlinear optical processes such as high harmonic generation, multiphoton absorption, and stimulated Raman scattering. We show, analytically and numerically, how a nonlinear optical process via resonance Raman scattering (RRS) can be manipulated in a four-level double-Λ system by using pulsed laser fields. We find that two simultaneously excited RRS paths involved in the system can generate an ultimately destructive interference in the broad-bandwidth-limit regime. This, in turn, reduces the four-level system to an equivalent three-level system in a *V* configuration capable of naturally vanishing RRS effects. We further show that this counterintuitive phenomenon, i.e., the RRS vanishing, can be prevented by transferring a modulated phase of the laser pulse to the system at resonance frequencies. This work demonstrates a clear signature of both quantum destructive and constructive interference by actively controlling resonant multiphoton processes in multilevel quantum systems, and it therefore has potential applications in nonlinear optics, quantum control, and quantum information science.

DOI: 10.1103/PhysRevLett.123.223202

Since C. V. Raman first reported the Raman effect in 1928 [1], Raman spectroscopy has been widely used for characterizing the low-lying energy levels of atoms [2], molecules [3], and low-dimensional nanomaterials [4]. When the wavelength of the incident light falls within an absorption band of interest, the Raman scattering efficiency can be significantly enhanced via a resonant two-photon process. This leads to resonance Raman scattering (RRS), which is more selective than its non-resonance Raman counterpart [5–8]. A RRS process requires a three-level system in a Λ configuration with two low-lying energy levels of the ground electronic state, and an intermediate energy level in the excited electronic state. Under certain conditions, such a three-level Λ model can be selectively isolated from quantum systems with complex energy structures, e.g., by using narrow-bandwidth lasers, and has been used as a standard model for studying various types of nonlinear optical schemes, including coherent population trapping [9,10], electromagnetically induced transparency [11–15], and stimulated Raman adiabatic passage [16–20]. However, when a pulsed laser field is applied with a broad bandwidth over multiple off-resonant levels, more than one RRS path will be activated. Therefore the complexity will be dramatically increased owing to the nonlinear optical effect via quantum coherence and interference within and between paths, leading to many unexpected quantum interference phenomena. This, in turn, opens a new avenue for studying these nonlinear effects via multiple-optical-path quantum interference. Understanding how the nonlinear effect can be affected and, ultimately, manipulated by applied external fields remains a long-standing goal of both fundamental and practical significance in quantum science and technology [21–27].

Here, we theoretically examine a multiple-optical-path quantum interference in a typical four-level double-Λ (FLDL) system with two low-lying energy levels of the ground electronic state and two low-lying energy levels of the excited electronic state. When such a quantum system interacts with a transform-limited (TL) pulse with a sufficiently broad bandwidth, we show that two simultaneously excited RRS paths can destructively interfere with each other, leading to a natural vanishing of the RRS phenomenon. We further find that this RRS vanishing can be prevented by modulating the spectral phase of the laser pulse at resonance frequencies. These findings not only deepen our understanding of quantum interference but also demonstrate an active way of manipulating nonlinear

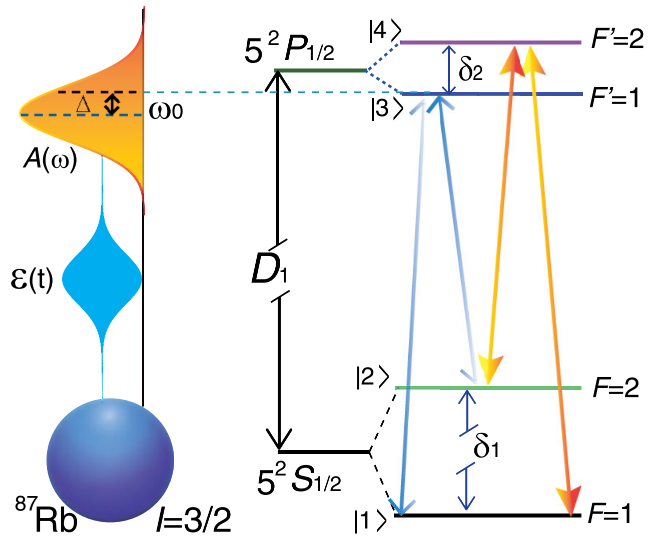

FIG. 1. Schematic of laser-induced RRS in a four-level double-Λ ^{87}Rb atom. The system consists of the hyperfine levels $F = 1$ and 2 of $5^2S_{1/2}$ with $\delta_1 = 6.8347$ GHz, and $F' = 1$ and 2 of $5^2P_{1/2}$ with $\delta_2 = 0.81656$ GHz. The four hyperfine levels are denoted by $|1\rangle, |2\rangle, |3\rangle$, and $|4\rangle$, and Δ corresponds to the detuning of ω_0 to the transition frequency between states $|1\rangle$ and $|3\rangle$.

optical processes in multilevel quantum systems, which is a topic of much current interest in quantum coherent control, quantum optics, and quantum information processing [28–35].

As a proof of principle, we consider a prototype system of an ultracold ^{87}Rb atom interacting with a pulsed laser field $\mathcal{E}(t)$ for exciting the optical D_1 transition; see Fig. 1, in which the system of Rb atoms is assumed to be in an ultracold dilute gas (e.g., via a magneto-optical trap [36,37]) to eliminate the Doppler shift of the laser field. Because of the interaction of the nuclear angular momentum and the electronic total angular moment, a hyperfine structure occurs, generating the hyperfine levels $F = 1$ and 2 of $5^2S_{1/2}$, with an energy split of $\delta_1 = 6.8347$ GHz, and the hyperfine levels $F' = 1$ and 2 of $5^2P_{1/2}$, with an energy split of $\delta_2 = 0.81656$ GHz. As indicated in Fig. 1, we use the states $|1\rangle, |2\rangle, |3\rangle$, and $|4\rangle$ with energies E_1, E_2, E_3, and E_4 to denote the four hyperfine levels, respectively. The evolution of the system from an initial time t_0 to a given time t can be described by using the unitary operator $U(t, t_0)$ with $U(t_0, t_0) \equiv \mathbb{I}$, and a solution of $U(t, t_0)$ can be written as ($\hbar = 1$)

$$U(t, t_0) = U(t_0, t_0) - i\int_{t_0}^{t} dt' H_I(t')U(t', t_0), \qquad (1)$$

where $H_I(t) = \exp(iH_0t)[-\hat{\mu}\mathcal{E}(t)]\exp(-iH_0t)$ in the interaction picture, with $\hat{H}_0 = \sum_{n=1}^{4} |n\rangle E_n\langle n|$ and $\mu_{nn'} = \langle n'|\hat{\mu}|n\rangle$ as the matrix elements of the dipole operator $\hat{\mu}$. For an initial condition of $|\psi(t_0)\rangle = |1\rangle$, the time-dependent wave function reads $|\psi(t)\rangle = U(t, t_0)|1\rangle$. Note that the dipole-allowed transitions between magnetic sublevels m_F and $m_{F'}$ of the hyperfine levels F and F' obey the selection rule $\Delta m_F = 0$ for a linearly polarized laser field. In our simulations, we consider the initial state $|1\rangle$ in $m_F = 1$ (which can be selected by using an optical pumping technique [38]), and therefore a FLDL configuration can be isolated from the full set of atomic transitions.

The FLDL system in Fig. 1 includes two RRS paths from $|1\rangle$ to $|2\rangle$ through either $|3\rangle$ or $|4\rangle$. By Magnus expanding $U(t, t_0)$ to first order [39], an analytic solution of a three-level Λ system with states $|1\rangle$, $|2\rangle$, and $|m\rangle$ ($m = 3$ or 4) driven by a linearly polarized laser pulse $\mathcal{E}(t)$ can be given by [40,41]

$$|\psi_{12m}^{(1)}(t)\rangle = \frac{|\theta_{2m}(t)|^2 + |\theta_{1m}(t)|^2\cos[\theta_{12m}(t)]}{|\theta_{12m}(t)|^2}|1\rangle + \frac{\theta_{1m}(t)\theta_{2m}^*(t)}{|\theta_{12m}(t)|^2}[\cos\theta_{12m}(t) - 1]|2\rangle + \frac{i\theta_{1m}(t)\sin\theta(t)}{\theta_{12m}(t)}|m\rangle, \qquad (2)$$

where the complex field areas $\theta_{1m}(t) = \mu_{1m}\int_0^t dt'\mathcal{E}(t')e^{-i\omega_{1m}t'}$, $\theta_{2m}(t) = \mu_{2m}\int_0^t dt'\mathcal{E}(t')e^{-i\omega_{2m}t'}$, and $\theta_{1m2}(t) = \sqrt{|\theta_{1m}(t)|^2 + |\theta_{2m}(t)|^2}$, with $\omega_{1m} = (E_m - E_1)$ and $\omega_{2m} = (E_m - E_2)$. For a broad-bandwidth pulse with $\Delta\omega > \delta_1$, state $|2\rangle$ is accessible via RRS. For a narrow-bandwidth pulse with $\Delta\omega \ll \delta_1$, however, the three-level system reduces to a two-level system with $|\psi_{1m}^{(1)}(t)\rangle = \cos[\theta(t)]|1\rangle + i\sin[\theta(t)]|m\rangle$, i.e., $\theta(t) = \theta_{1m}(t)$ without the RRS to $|2\rangle$.

To show the dependence of the RRS on $\Delta\omega$, we consider $\mathcal{E}(t) = \mathrm{Re}[(1/2\pi)\int_0^\infty A(\omega)e^{i[\phi(\omega)-\omega t]}d\omega]$, with spectral amplitude $A(\omega) = (A_0/\mu_{1m})\exp[\{-(\omega-\omega_0)^2/2(\Delta\omega)^2\}]$, to excite a three-level system of $|1\rangle$, $|2\rangle$, and $|m\rangle$. For this choice, the pulse area at t_f, i.e., $\theta_{1m}(t_f)$ [$\propto A(\omega_{1m})$], is independent of $\Delta\omega$ for a given A_0 at $\omega_0 = \omega_{1m}$. As an example, we demonstrate such excitations in a three-level system of $|1\rangle$, $|2\rangle$, and $|3\rangle$, by excluding state $|4\rangle$, and numerically solve the corresponding equation (1) to calculate the wave function $|\psi_{123}(t)\rangle$. Figures 2(a) and 2(b) show a comparison of the numerically (exactly) calculated populations $P_n(t_f) = |\langle n|\psi_{123}(t_f)\rangle|^2$ with the analytically derived populations $P_n^{(1)}(t_f) = |\langle n|\psi_{123}^{(1)}(t_f)\rangle|^2$ ($n = 2, 3$) versus $\Delta\omega$. We choose $A_0 = \pi/4$ and keep $\phi(\omega) = 0$, which, using Eq. (2), will fix $\theta_{13}(t_f) = \pi/4$ and lead to an equal population distribution between $|1\rangle$ and $|3\rangle$ in a narrow-bandwidth regime of $\Delta\omega \ll \delta_1$; see Figs. 2(a) and 2(b). The quantum state transfer (QST) to $|2\rangle$ appears in the three-level numerical (3LN) simulations as the bandwidth increases and asymptotically approaches a constant in the broad-bandwidth-limit regime, in good agreement with the three-level analytical (3LA) solutions.

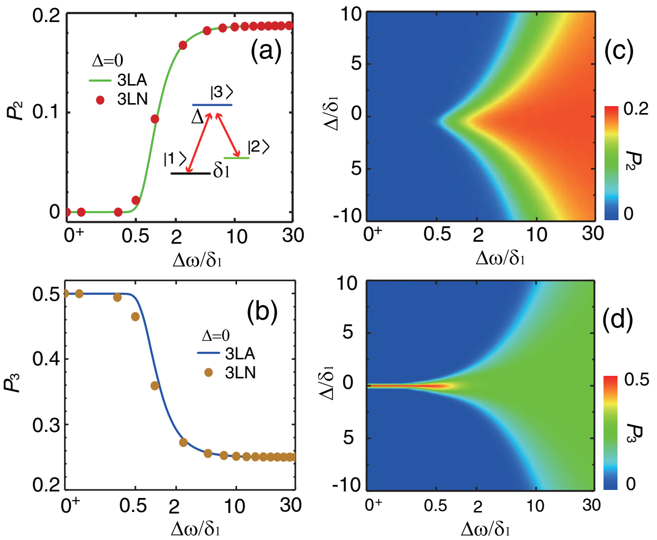

FIG. 2. The presence of resonance Raman scattering in a three-level Λ system. (a),(b) Final populations $P_2(t_f)$ and $P_3(t_f)$ versus $\Delta\omega$ based on the three-level numerical (3LN) solutions at the resonant condition $\Delta = 0$, which are compared with the three-level analytical (3LA) solutions. (c),(d) The dependence of $P_2(t_f)$ and $P_3(t_f)$ on both $\Delta\omega$ and Δ. The three-level Λ system used in simulations is shown in (a).

We further consider the effect of $\Delta = \omega_0 - \omega_{13}$ on the RRS; see Figs. 2(c) and 2(d). The detuning hampers the QST efficiency to $|2\rangle$, whereas it remains visible in the region $\Delta\omega > \Delta$. We also examine the same simulations for another RRS path from $|1\rangle$ to $|2\rangle$ through $|4\rangle$ by excluding $|3\rangle$, and we find results similar to those in Fig. 2. These simulations strongly support the RRS presence in the three-level Λ system driven by a laser pulse with sufficiently broad bandwidths.

We now focus on the FLDL system by considering the two closely spaced states $|3\rangle$ and $|4\rangle$ connected to $|1\rangle$ and $|2\rangle$. Figure 3(a) shows the dependence of $P_2(t_f) = |\langle 2|\psi(t_f)\rangle|^2$ on $\Delta\omega$, for which the wave function $|\psi(t)\rangle$ is obtained by numerically solving Eq. (1) with the FLDL model while using the same pulse as that in Fig. 2.

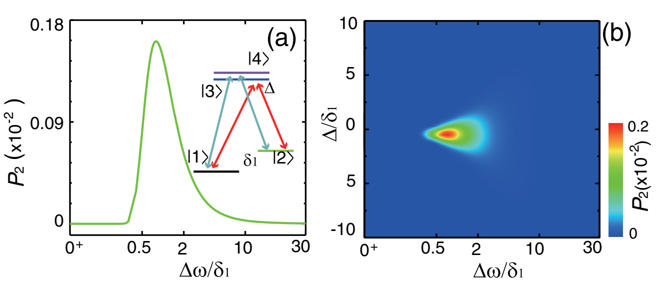

FIG. 3. The vanishing of the resonance Raman scattering in the FLDL system. (a) The numerically calculated population $P_2(t_f) = |\langle 2|\psi(t_f)\rangle|^2$ versus $\Delta\omega$ at $\Delta = 0$. (Inset) The FLDL system used in the simulations. (b) The final population $P_2(t_f)$ versus both $\Delta\omega$ and Δ.

Surprisingly, QST to $|2\rangle$ reaches a maximal value of 0.15% only around $\Delta\omega = 1.0\delta_1$ and then decreases to a value of $< 10^{-4}$ in the broad-bandwidth-limit regime. Figure 3(b) shows the dependence of $P_2(t_f)$ on both $\Delta\omega$ and Δ. The transition probability to $|2\rangle$ still remains extremely small, $< 10^{-4}$, even for a larger detuning. This implies that the RRS to $|2\rangle$ is significantly suppressed in the FLDL system.

We first analyze the pulse area theorem with Eq. (2) to qualitatively understand the underlying mechanism in Fig. 3. Since the energy splitting between $|3\rangle$ and $|4\rangle$ is extremely small, the variations of the $A(\omega)$ used at ω_{1m} and ω_{2m} can be ignored in the limit regime of $\Delta\omega \gg \delta_1$, i.e., $A(\omega_{13}) \approx A(\omega_{14})$ and $A(\omega_{23}) \approx A(\omega_{24})$. This implies that the values of $\theta_{1m}(t_f)$ and $\theta_{2m}(t_f)$ are determined by the values of $\mu_{13}, \mu_{23}, \mu_{14}$, and μ_{24}. According to Refs. [42,43], there is a geometrical structure of $\mu_{13} = -\sqrt{1/3}\mu_{14}$, $\mu_{23} = \mu_{14}$, and $\mu_{24} = \sqrt{1/3}\mu_{14}$, leading to the relation $\theta_{13}(t_f)\theta^*_{23}(t_f) \approx -\theta_{14}(t_f)\theta^*_{24}(t_f)$. When the complex pulse areas further satisfy the condition $|\theta_{132}(t_f)| \approx |\theta_{142}(t_f)|$, the two simultaneously excited RRS processes cancel each other out by using the TL pulse.

To further gain insights into the RRS vanishing in Fig. 3, we derive a pulse area theorem for the FLDL system driven by a pulsed field in the broad-bandwidth-limit regime (see the details in the Supplemental Material [44]). The time-dependent wave function of the system reads

$$|\psi^{(1)}(t)\rangle = \cos[\theta(t)]|1\rangle + \frac{i\theta_1(t)}{2\theta(t)}\sin[\theta(t)]|3\rangle + \frac{i\sqrt{3}\theta_1(t)}{2\theta(t)}\sin[\theta(t)]|4\rangle, \quad (3)$$

with $\theta_1(t) = 2\theta_{13}(t)$ and $\theta(t) = |\theta_1(t)|$. The FLDL system is reduced into a three-level system in a V configuration without QST to $|2\rangle$ at any time t, corresponding to the counterintuitive phenomenon of the RRS vanishing. Note that the derivation of Eq. (3) does not require the strict condition $|\theta_{132}(t_f)| \approx |\theta_{142}(t_f)|$ for generating the RRS vanishing. The analytical solution in Eq. (3) is valid only in the broad-bandwidth-limit regime. In the narrow-bandwidth regime, however, the two RRS paths will be naturally closed, corresponding to a three-level V system, which has an analytical solution [40]

$$|\psi^{(1)}_{134}(t)\rangle = \cos[\theta(t)]|1\rangle + \frac{i\theta_{13}(t)}{\theta(t)}\sin[\theta(t)]|3\rangle + \frac{i\theta_{14}(t)}{\theta(t)}\sin[\theta(t)]|4\rangle \quad (4)$$

with $\theta(t) = \sqrt{|\theta_{13}(t)|^2 + |\theta_{14}(t)|^2}$. Clearly, the two three-level solutions by Eqs. (3) and (4) contain different physical meanings, but it is interesting that Eq. (4) is equivalent to

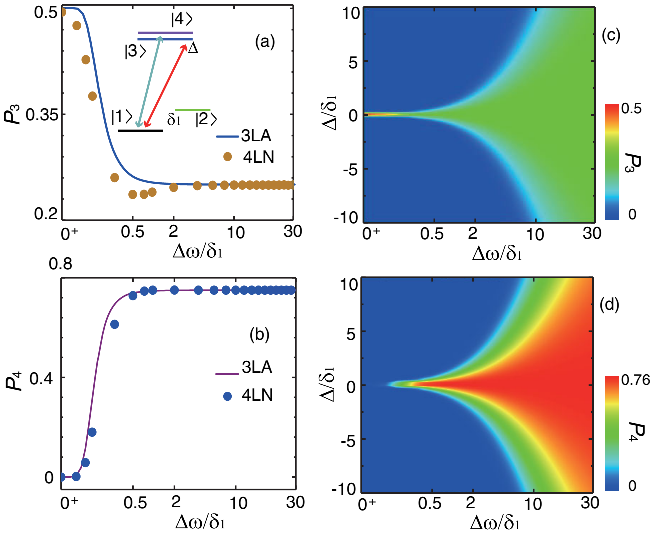

FIG. 4. The vanishing of resonance Raman scattering in the FLDL system. (a),(b) The final populations $P_3(t_f)$ and $P_4(t_f)$ versus $\Delta\omega$ at $\Delta = 0$ based on the four-level numerical (4LN) solutions, which are compared with that by using the 3LA solutions. [Inset in (a)] The FLDL system and the equivalent three-level V system used in simulations. (c),(d) The calculated final populations $P_3(t_f)$ and $P_4(t_f)$ versus both $\Delta\omega$ and Δ.

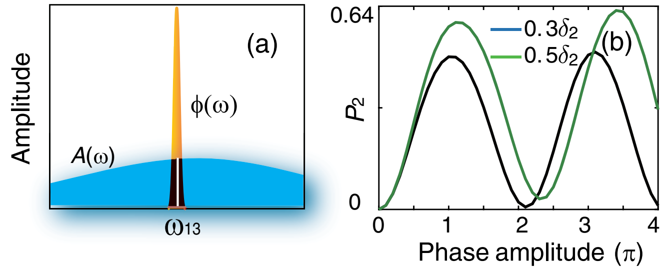

FIG. 5. The RRS revival in the FLDL system. (a) Schematic of a Gaussian phase modulation with a function $\phi(\omega) = a\exp[-(\omega-\omega_c)^2/2b^2]$ (orange) centered at $\omega_c = \omega_{13}$ with a width of b in the broad-bandwidth-limit regime, and of a Gaussian spectral amplitude $A(\omega)$ (blue). (b) The corresponding final population $P_2(t_f)$ versus the phase amplitude a from 0 to 4π for two different widths of $b = 0.3\delta_2$ (black line) and $b = 0.5\delta_2$ (green line).

Eq. (3) in the broad-bandwidth-limit regime by inserting $\omega_{13} = \omega_{14}$ into Eq. (4). There is a pulse area theorem of $\theta(t_f) = \pi/2$ [i.e., $\theta_{13}(t_f) = \pi/4$], capable of achieving a complete QST from $|1\rangle$ to upper states with 25% in $|3\rangle$ and 75% in $|4\rangle$ (see the details in the Supplemental Material [44]).

Figure 4 shows a comparison of the four-level numerical (4LN) simulations with the 3LA solutions by Eq. (4) and plots the final populations in $|3\rangle$ and $|4\rangle$ versus $\Delta\omega$ and Δ. As can be seen from Figs. 4(a) and 4(b), the 4LN results can be reproduced with high precision by using the 3LA solutions. Both approaches converge to the theoretical values of $P_3 = 25\%$ and $P_4 = 75\%$, in good agreement with the pulse area theorem by Eq. (3). A slight difference can be attributed to the breakdown of $A(\omega_{13}) \approx A(\omega_{14})$ and $A(\omega_{23}) \approx A(\omega_{24})$ in the narrow-bandwidth regime. The dependence of $P_3(t_f)$ and $P_4(t_f)$ on both $\Delta\omega$ and Δ in Figs. 4(c) and 4(d) demonstrates that the RRS vanishing can be robustly observed in a broad region of $(\Delta\omega, \Delta)$ in the FLDL system. The detuning only decreases the efficiency of the population transfer to $|3\rangle$ and $|4\rangle$, but it does not destroy the RRS vanishing.

We finally present an approach to revive the RRS by modulating the sign of $\theta_{13}(t_f)\theta_{23}^*(t_f)$ [or $\theta_{14}(t_f)\theta_{24}^*(t_f)$] in Eq. (2) so that both RRS paths can constructively interfere with each other. The direct application of a π phase shift at the resonance frequencies will lead to an infinitely long pulse. In order to reduce the computational cost, we instead apply a Gaussian phase function $\phi(\omega) = a\exp[-(\omega-\omega_c)^2/2b^2]$, centered at ω_c to a very small window of width $b < \delta_2$, while fixing $A(\omega)$ unchanged, as illustrated in Fig. 5(a). This corresponds to a coherent optical-phase modulation of nonlinear optical processes by using the current broad-bandwidth pulse shaping technique [45,46], which has been successfully demonstrated in several seminal experiments [43,47]. Figure 5(b) shows a simulation of $P_2(t_f)$ versus a from 0 to 4π by setting $\omega_c = \omega_{13}$, which can invert the sign of $\theta_{13}(t_f)\theta_{23}^*(t_f)$ with $a = \pi$ while keeping the sign of $\theta_{14}(t_f)\theta_{24}^*(t_f)$ unchanged. Two different widths of $b = 0.3\delta_2$ and $0.5\delta_2$ are examined for the case of $\Delta\omega \approx 23\delta_1$, which can significantly prolong the shaped laser pulse with a length of $(t_f - t_0) > 10$ ns. A clear dependence of $P_2(t_f)$ on the phase amplitude appears with a maximum of $P_2(t_f) = 0.4864$ at $a = \pi$ for $b = 0.3\delta_2$, indicating that the RRS can be manipulated by modulating the spectral phase at resonance frequencies. This enhancement approach differs from Refs. [43,47] by modulating the nonresonant spectral components of the pulses.

The RRS enhancements in Fig. 5(b) exhibit another maximum of $P_2(t_f) = 0.4955$ at $a = 3.1\pi$ with a small shift from 3π. All maximums become slightly higher than 0.4752 by directly inverting the sign of μ_{13} and do not decrease to the minimum exactly at 2π and 4π. These differences imply that the Gaussian phase with a width also modulates the spectral components around ω_{13}, leading to the interference of RRS with the detuned RRS. As a result, the RRS manipulation via this Gaussian phase modulation depends on the actual width of the phase function. A broad width of phase function with $b = 0.5\delta_2$ increases the enhancement in Fig. 5(b), indicating that the deturned-RRS paths play roles and constructively interfere with the RRS paths.

In summary, we theoretically examined a nonlinear optical effect via multiple-optical-path quantum interference in a FLDL ^{87}Rb at ultracold temperatures. We found that a robust phenomenon of the RRS vanishing can be generated by using a TL pulse in the broad-bandwidth-limit regime. By transferring a modulated spectral phase of the laser pulse onto the system, we demonstrated that this counterintuitive phenomenon of the RRS vanishing could be prevented, leading to the RRS revival. This work provides a clear signature of both destructive and constructive interference toward ultimately manipulating resonant multiphoton optical processes in ultracold ^{87}Rb atoms.

Ultracold ^{87}Rb was the first and is the most popular atom for making Bose-Einstein condensates. This atom with excellent sensitivity is also studied for atomic clocks [48], quantum Raman memory [49], quantum sensors [50], quantum gate [51], and atom interferometers [52]. Our results contribute a new physical phenomenon to ^{87}Rb and stimulated Raman scattering for exploiting nonlinear optical effects. The RRS vanishing within the present model requires the complex field areas to satisfy the condition $\theta_{13}(t_f)\theta_{23}^*(t_f) \approx -\theta_{14}(t_f)\theta_{24}^*(t_f)$ in the broad-bandwidth-limit regime. According to Ref. [42], this condition is generally applicable to ^{87}Rb (as well as to other alkali metal atoms) initially in a pure m_F magnetic sublevel. It implies that the RRS vanishing also occurs for the system initially in a hyperfine level F (in the absence of optical pumping). For a quantum system without the dipole relation as ^{87}Rb atom, an optimized spectral phase could be designed to either suppress or enhance the RRS processes [53–56]. Since atomic and optical physics can also be demonstrated in artificial quantum systems such as superconducting circuits [57,58], and charged nitrogen or silicon vacancy center in diamond [59–61], we expect that this RRS manipulation can be applied to solid-state systems with potential applications to quantum information and quantum computing science [62–66].

This work was supported in part by the National Natural Science Foundation of China (NSFC) under Grants No. 61973317 and No. 61828303, and by the Australian Research Council's Discovery Projects Funding Scheme under Project No. DP190101566. D. D. is supported in part by the U.S. Office of Naval Research Global under Grant No. N62909-19-1-2129. F. N. is supported in part by the MURI Center for Dynamic Magneto-Optics via the Air Force Office of Scientific Research (AFOSR) (Grant No. FA9550-14-1-0040), Army Research Office (ARO) (Grant No. W911NF-18-1-0358), Asian Office of Aerospace Research and Development (AOARD) (Grant No. FA2386-18-1-4045), Japan Science and Technology Agency (JST) (via the Q-LEAP program, and CREST Grant No. JPMJCR1676), Japan Society for the Promotion of Science (JSPS) (JSPS-RFBR Grant No. 17-52-50023, and JSPS-FWO Grant No. VS.059.18N), the RIKEN-AIST Challenge Research Fund, the FQXi Foundation, and the NTT PHI labs. C.-C. S. acknowledges the support and hospitality provided by RIKEN during his visit.

*cc.shu@csu.edu.cn

[1] C. V. Raman and K. S. Krishnan, A new type of secondary radiation, Nature (London) **121**, 501 (1928).

[2] C. Solaro, S. Meyer, K. Fisher, M. V. DePalatis, and M. Drewsen, Direct Frequency-Comb-Driven Raman Transitions in the Terahertz Range, Phys. Rev. Lett. **120**, 253601 (2018).

[3] S. C. Epstein, A. R. Huff, E. S. Winesett, C. H. Londergan, and L. K. Charkoudian, Tracking carrier protein motions with Raman spectroscopy, Nat. Commun. **10**, 2227 (2019).

[4] A. Eckmann, A. Felten, A. Mishchenko, L. Britnell, R. Krupke, K. S. Novoselov, and C. Casiraghi, Probing the nature of defects in graphene by Raman spectroscopy, Nano Lett. **12**, 3925 (2012).

[5] J. R. Simpson, O. Roslyak, J. G. Duque, E. H. Hároz, J. J. Crochet, H. Telg, A. Piryatinski, A. Walker, and S. K. Doorn, Resonance Raman signature of intertube excitons in compositionally-defined carbon nanotube bundles, Nat. Commun. **9**, 637 (2018).

[6] E. V. Efremov, F. Ariese, and C. Gooijer, Achievements in resonance Raman spectroscopy: Review of a technique with a distinct analytical chemistry potential, Anal. Chim. Acta **606**, 119 (2008).

[7] J. G. Duque, H. Telg, H. Chen, A. K. Swan, A. P. Shreve, X. Tu, M. Zheng, and S. K. Doorn, Quantum Interference Between the Third and Fourth Exciton States in Semiconducting Carbon Nanotubes Using Resonance Raman Spectroscopy, Phys. Rev. Lett. **108**, 117404 (2012).

[8] A. Materny, T. Chen, A. Vierheilig, and W. Kiefer, A review on linear and non-linear resonance Raman spectroscopy of the conjugated system polydiacetylene, J. Raman Spectrosc. **32**, 425 (2001).

[9] P. Jamonneau, G. Hétet, A. Dréau, J.-F. Roch, and V. Jacques, Coherent Population Trapping of a Single Nuclear Spin Under Ambient Conditions, Phys. Rev. Lett. **116**, 043603 (2016).

[10] A. Donarini, M. Niklas, M. Schafberger, N. Paradiso, C. Strunk, and M. Grifoni, Coherent population trapping by dark state formation in a carbon nanotube quantum dot, Nat. Commun. **10**, 381 (2019).

[11] M. Fleischhauer, A. Imamoglu, and J. P. Marangos, Electromagnetically induced transparency: Optics in coherent media, Rev. Mod. Phys. **77**, 633 (2005).

[12] Y. Guo, L. Zhou, L. M. Kuang, and C. P. Sun, Magneto-optical Stern-Gerlach effect in an atomic ensemble, Phys. Rev. A **78**, 013833 (2008).

[13] B. Peng, S. K. Ozdemir, W. Chen, F. Nori, and L. Yang, What is and what is not electromagnetically induced transparency in whispering-gallery microcavities, Nat. Commun. **5**, 5082 (2014).

[14] X. Gu, S. N. Huai, F. Nori, and Y. X. Liu, Polariton states in circuit QED for electromagnetically induced transparency, Phys. Rev. A **93**, 063827 (2016).

[15] J. Long, H. S. Ku, X. Wu, X. Gu, R. E. Lake, M. Bal, Y.-X. Liu, and D. P. Pappas, Electromagnetically Induced Transparency in Circuit Quantum Electrodynamics with Nested Polariton States, Phys. Rev. Lett. **120**, 083602 (2018).

[16] L. F. Wei, J. R. Johansson, L. X. Cen, S. Ashhab, and F. Nori, Controllable Coherent Population Transfers in

Superconducting Qubits for Quantum Computing, Phys. Rev. Lett. **100**, 113601 (2008).

[17] G. Falci, P. G. Di Stefano, A. Ridolfo, A. D'Arrigo, G. S. Paraoanu, and E. Paladino, Advances in quantum control of three-level superconducting circuit architectures, Fortschr. Phys. **65**, P1600077 (2017).

[18] C.-C. Shu, J. Yu, K.-J. Yuan, W.-H. Hu, J. Yang, and S.-L. Cong, Stimulated Raman adiabatic passage in molecular electronic states, Phys. Rev. A **79**, 023418 (2009).

[19] K. S. Kumar, A. Vepsäläinen, S. Danilin, and G. S. Paraoanu, Stimulated Raman adiabatic passage in a three-level superconducting circuit, Nat. Commun. **7**, 10628 (2016).

[20] N. V. Vitanov, A. A. Rangelov, B. W. Shore, and K. Bergmann, Stimulated Raman adiabatic passage in physics, chemistry, and beyond, Rev. Mod. Phys. **89**, 015006 (2017).

[21] M. Shapiro and P. Brumer, Coherent control of atomic, molecular, and electronic processes, Adv. At. Mol. Opt. Phys. **42**, 287 (2000).

[22] M. Dantus, Coherent nonlinear spectroscopy: From femtosecond dynamics to control, Annu. Rev. Phys. Chem. **52**, 639 (2001).

[23] Y. Silberberg, Quantum coherent control for nonlinear spectroscopy and microscopy, Annu. Rev. Phys. Chem. **60**, 277 (2009).

[24] J. D. Pritchard, K. J. Weatherill, and C. S. Adams, Nonlinear optics using cold Rydberg atoms, Annu. Rev. Cold At. Mol. **1**, 301 (2013).

[25] Z. L. Xiang, S. Ashhab, J. Q. You, and F. Nori, Hybrid quantum circuits: Superconducting circuits interacting with other quantum systems, Rev. Mod. Phys. **85**, 623 (2013).

[26] S. J. Glaser, U. Boscain, T. Calarco, C. P. Koch, W. Köckenberger, R. Kosloff, I. Kuprov, B. Luy, S. Schirmer, T. Schulte-Herbrüggen, D. Sugny, and F. K. Wilhelm, Training Schrödinger's cat: quantum optimal control, Eur. Phys. J. D **69**, 279 (2015).

[27] J. Zhang, Y. X. Liu, R. B. Wu, K. Jacobs, and F. Nori, Quantum feedback: theory, experiments, and applications, Phys. Rep. **679**, 1 (2017).

[28] A. C. Han and M. Shapiro, Linear Response in the Strong Field Domain, Phys. Rev. Lett. **108**, 183002 (2012).

[29] A. Konar, V. V. Lozovoy, and M. Dantus, Solvation stokes-shift dynamics studied by chirped femtosecond laser pulses, J. Phys. Chem. Lett. **3**, 2458 (2012).

[30] A. J. Traverso, B. Hokr, Z. Yi, L. Yuan, S. Yamaguchi, M. O. Scully, and V. V. Yakovlev, Two-Photon Infrared Resonance can Enhance Coherent Raman Scattering, Phys. Rev. Lett. **120**, 063602 (2018).

[31] X. Gu, A. F. Kockum, A. Miranowicz, Y. X. Liu, and F. Nori, Microwave photonics with superconducting quantum circuits, Phys. Rep. **718–719**, 1 (2017).

[32] A. F. Kockum, A. Miranowicz, V. Macrì, S. Savasta, and F. Nori, Deterministic quantum nonlinear optics with single atoms and virtual photons, Phys. Rev. A **95**, 063849 (2017).

[33] K. Wilma, C.-C. Shu, U. Scherf, and R. Hildner, Visualizing hidden ultrafast processes in individual molecules by single-pulse coherent control, J. Am. Chem. Soc. **140**, 15329 (2018).

[34] L. Liu, D.-C. Zhang, H. Yang, Y.-X. Liu, J. Nan, J. Rui, B. Zhao, and J.-W. Pan, Observation of Interference Between Resonant and Detuned Stirap in the Adiabatic Creation of ^{23}Na^{40}K Molecules, Phys. Rev. Lett. **122**, 253201 (2019).

[35] C.-H. Wu, C.-K. Liu, Y.-C. Chen, and C.-S. Chuu, Revival of Quantum Interference by Modulating the Biphotons, Phys. Rev. Lett. **123**, 143601 (2019).

[36] E. L. Raab, M. Prentiss, A. Cable, S. Chu, and D. E. Pritchard, Trapping of Neutral Sodium Atoms with Radiation Pressure, Phys. Rev. Lett. **59**, 2631 (1987).

[37] A. Marian, M. C. Stowe, J. R. Lawall, D. Felinto, and J. Ye, United time-frequency spectroscopy for dynamics and global structure, Science **306**, 2063 (2004).

[38] W. Happer, Optical pumping, Rev. Mod. Phys. **44**, 169 (1972).

[39] S. Blanes, F. Casas, J. A. Oteo, and J. Ros, The Magnus expansion and some of its applications, Phys. Rep. **470**, 151 (2009).

[40] G. Shchedrin, C. O'Brien, Y. Rostovtsev, and M. O. Scully, Analytic solution and pulse area theorem for three-level atoms, Phys. Rev. A **92**, 063815 (2015).

[41] Y. Guo, X. B. Luo, S. Ma, and C.-C. Shu, All-optical generation of quantum entangled state with strict constrained ultrafast laser pulses, Phys. Rev. A **100**, 023409 (2019).

[42] D. A. Steck, Rubidium 87 D Line Data, http://steck.us/alkalidata/rubidium87numbers.pdf.

[43] M. C. Stowe, A. Pe'er, and J. Ye, Control of Four-Level Quantum Coherence via Discrete Specral Shaping of an Optical Frequency Comb, Phys. Rev. Lett. **100**, 203001 (2008).

[44] See Supplemental Material at http://link.aps.org/supplemental/10.1103/PhysRevLett.123.223202 for the technical details for deriving Eq. (3) and the pulse area theorem for analyzing Fig. 4 in the main text.

[45] A. Monmayrant, S. Weber, and B. Chatel, A newcomer's guide to ultrashort pulse shaping and characterization, J. Phys. B **43**, 103001 (2010).

[46] A. M. Weiner, Femtosecond pulse shaping using spatial light modulators, Rev. Sci. Instrum. **71**, 1929 (2000).

[47] N. Dudovich, B. Dayan, S. M. Gallagher Faeder, and Y. Silberberg, Transform-Limited Pulses are not Optimal for Resonant Multiphoton Transitions, Phys. Rev. Lett. **86**, 47 (2001).

[48] L. Liu, D.-S. Lü, and Y.-Z. Wang, In-orbit operation of an atomic clock based on laser-cooled ^{87}Rb atoms, Nat. Commun. **9**, 2760 (2018).

[49] A. G. Radnaev, Y. O. Dudin, R. Zhao, H. H. Jen, S. D. Jenkins, A. Kuzmich, and T. A. B. Kennedy, A quantum memory with telecom-wavelength conversion, Nat. Phys. **6**, 894 (2010).

[50] X. Alauze, A. Bonnin, C. Solaro, and F. P. D. Santos, A trapped ultracold atom force sensor with a μm-scale spatial resolution, New J. Phys. **20**, 083014 (2018).

[51] Y. Zeng, P. Xu, X.-D. He, Y.-Y. Liu, M. Liu, J. Wang, D. J. Papoular, G. V. Shlyapnikov, and M.-S. Zhan, Entangling two Individual Atoms of Different Isotopes via Rydberg Blockade, Phys. Rev. Lett. **119**, 160502 (2017).

[52] L. Zhou, S.-T. Long, B. Tang, X. Chen, F. Gao, W.-C. Peng, W.-T. Duan, J.-Q. Zhong, Z.-Y. Xiong, J. Wang, Y.-Z. Zhang, and M.-S. Zhan, Test of Equivalence Principle at

10^{-8} Level by a Dual-Species Double-Diffraction Raman Atom Interferometer, Phys. Rev. Lett. **115**, 013004 (2015).
[53] R. S. Judson and H. Rabitz, Teaching Lasers to Control Molecules, Phys. Rev. Lett. **68**, 1500 (1992).
[54] C.-C. Shu, T.-S. Ho, X. Xing, and H. Rabitz, Frequency domain quantum optimal control under multiple constraints, Phys. Rev. A **93**, 033417 (2016).
[55] C.-C. Shu, D. Dong, I. R. Petersen, and N. E. Henriksen, Complete elimination of nonlinear light-matter interactions with broadband ultrafast laser pulses, Phys. Rev. A **95**, 033809 (2017).
[56] Y. Guo, D. Dong, and C.-C. Shu, Optimal and robust control of quantum state transfer by shaping spectral phase of ultrafast laser pulses, Phys. Chem. Chem. Phys. **20**, 9498 (2018).
[57] J. Q. You and F. Nori, Atomic physics and quantum optics using superconducting circuits, Nature (London) **474**, 589 (2011).
[58] Y. X. Liu, J. Q. You, L. F. Wei, C. P. Sun, and F. Nori, Optical Selection Rules and Phase-Dependent Adiabatic State Control in a Superconducting Quantum Circuit, Phys. Rev. Lett. **95**, 087001 (2005).
[59] E. Togan, Y. Chu, A. S. Trifonov, L. Jiang, J. Maze, L. Childress, M. V. G. Dutt, A. S. Sørensen, P. R. Hemmer, A. S. Zibrov, and M. D. Lukin, Quantum entanglement between an optical photon and a solid-state spin qubit, Nature (London) **466**, 730 (2010).
[60] D. M. Toyli, D. J. Christle, A. Alkauskas, B. B. Buckley, C. G. Van de Walle, and D. D. Awschalom, Measurement and Control of Single Nitrogen-Vacancy Center Spins above 600 K, Phys. Rev. X **2**, 031001 (2012).
[61] J. N. Becker, J. Görlitz, C. Arend, M. Markham, and C. Becher, Ultrafast all-optical coherent control of single silicon vacancy colour centres in diamond, Nat. Commun. **7**, 13512 (2016).
[62] J. Buluta and F. Nori, Quantum simulators, Science **326**, 108 (2009).
[63] I. Buluta, S. Ashhab, and F. Nori, Natural and artificial atoms for quantum computation, Rep. Prog. Phys. **74**, 104401 (2011).
[64] I. M. Georgescu, S. Ashhab, and F. Nori, Quantum simulation, Rev. Mod. Phys. **86**, 153 (2014).
[65] P. Krantz, M. Kjaergaard, F. Yan, T. P. Orlando, S. Gustavsson, and W. D. Oliver, A quantum engineer's guide to superconducting qubits, Appl. Phys. Rev. **6**, 021318 (2019).
[66] J. F. Barry, J. M. Schloss, E. Bauch, M. J. Turner, C. A. Hart, L. M. Pham, and R. L. Walsworth, Sensitivity optimization for NV-diamond magnetometry, arXiv:1903.08176v1 [Rev. Mod. Phys. (to be published)].